Distributed nonlinear control for a microgrid embedding renewables, train's energy recovery system and storages

Alessio Iovine, Lilia Galai Dol, Gilney Damm, Elena de Santis, Maria Domenica Di Benedetto

Distributed Nonlinear Control for a MicroGrid Embedding Renewables, Train's Energy Recovery System and Storages

Alessio Iovine, Efficacity, France, a.iovine@efficacity.com
Lilia Galai Dol, Efficacity, France, l.galai-dol@efficacity.com
Gilney Damm, Laboratoire IBISC, Paris-Saclay University, France, gilney.damm@ibisc.fr
Elena De Santis, L'Aquila University, Italy, elena.desantis@univaq.it
Maria Domenica Di Benedetto, L'Aquila University, Italy, mariadomenica.dibenedetto@univaq.it

The Presentation pdf file will be available after the conference.

Abstract

A low-level distributed nonlinear controller for a DC MicroGrid integrated in a Train Station is introduced in this paper. A number of elements are connected to the MicroGrid: two different transient time scale renewables (braking recovery and photovoltaic), two kinds of storage acting at different time-scale (a battery and a supercapacitor), and a load. The model is developed and a complete stability analysis is investigated: power balance and voltage grid stability requirements are both met. A System of Systems approach is utilized to develop the control laws for the DC/DC converters in order to fulfil the dedicated objective each controller has. Simulation results showing the desired grid behaviour are presented.

1. Introduction

Direct Current (DC) microgrids are attracting interest thanks to their ability to easily integrate modern loads, renewable sources and energy storages [1], [2], [3], [4], [5]. They also acknowledged the fact that most renewable energy sources and storage use DC energy (as photovoltaics and batteries for example), and allow the reduction of the number of power converters in the grid. By doing this, they reduce losses, and allow fast control of the grid. This is capital to comply to the fast variations intrinsic to renewables [6].

Nowadays, energy coming from renewable sources (renewables) can be stored for future utilization or sent to the main AC grid even if these energies are intermittent thanks to storage devices utilization. All except braking energy recovery, which has not been studied so far. A train station dedicated DC MicroGrid is here introduced: the microgrid's targets are to merge residual braking energy recovered from the trains to that produced by photovoltaics and to maintain a desired voltage level. It is considered a framework of two different storage systems with different targets in order to have energy reservoir when needed as well as being able to absorb sufficiently fast power coming from the braking system, and to make the DC grid resilient to disturbances or transient phenomena, using two different time scales. The adopted scheme is depicted in Fig. 1.

This paper is organized as follows. In Section 2 the model of the DC MicroGrid is introduced. Then in Section 3 the adopted analysis is carried out to satisfy stability requirements. Section 4 provides simulation results, while in Section 5 conclusions are provided.

2. DC MicroGrid design in station neighbourhood

The considered MicroGrid is a DC one without a connection to a main AC grid. A corresponding scheme to better describing the general one introduced in Fig. 1 is depicted in Fig. 2.

The target is to assure voltage stability in the DC grid and correctly feed power to the load while absorbing power from the PV array and the braking energy recovery system. To each component of the microgrid (PV array, energy recovery system, battery, supercapacitor) a DC/DC converter is connected. Furthermore, another important target is to save battery lifetime. Since the braking energy recovery system introduces a high level of current in a

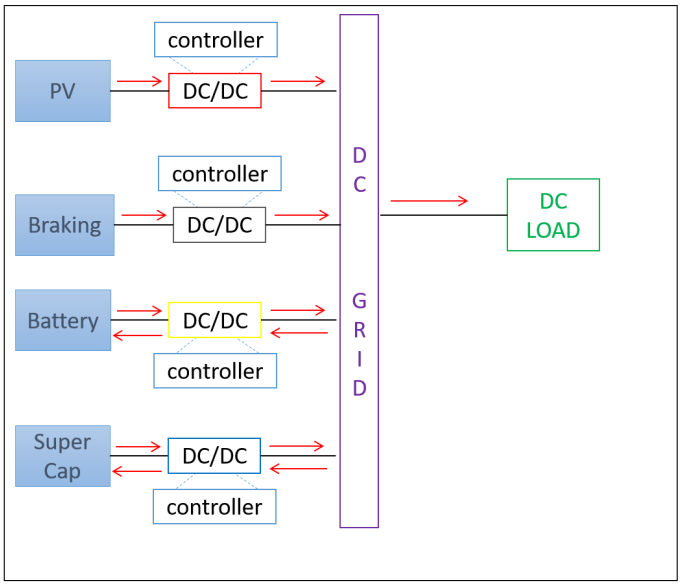

Figure 1: The considered framework: An illustrative scheme.

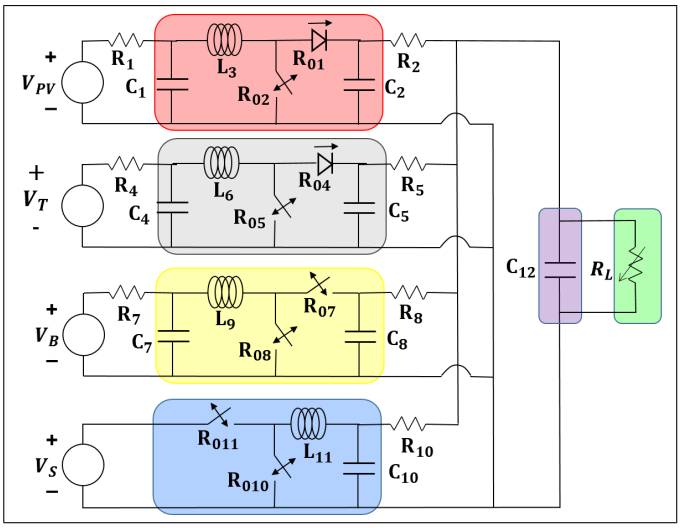

Figure 2: The considered framework: A circuital scheme.

short time period, the battery would result stressed and its lifetime could be reduced if it would be in charge of absorbing this power. A supercapacitor is then selected to absorb that amount of power; indeed thanks to its different characteristics, its lifetime will not be affected as the battery. Power coming from the battery will then be modified according to the new level of energy in the supercapacitor, but according to a desired charge/discharge rate. Two assumptions are made. A higher level controller is supposed to provide references to be accomplished by the local controllers [7], [8], [9]; the second one is about a proper sizing of PV array, battery and supercapacitor in order to have feasible power balance with respect to the sizing of the load.

The voltage of the DC grid is influenced by the connection with load and sources. The DC/DC converter connecting the PV array to the DC grid is a boost one and it is illustrated in the red area in Fig. 2. Its target is to obtain the maximum amount of power from the PV array regulating the voltage v_{C_1} to its reference v_1^*, given by the higher level controller implementing Maximum Power Point Tracking (MPPT) algorithm, and considered constant during each time interval T. The DC/DC converter dedicated to energy recovery from the train braking is the boost one in grey in Fig. 2. Its target is to obtain energy from the increase of the voltage v_T when the train is breaking; so it assigns the value v_4^* to v_{C_4}, where v_4^* is the voltage level of v_T when there is no recovery energy from the train braking and consequently there is no current generated. The DC/DC converter connecting the battery is a bost-buck bidirectional converter (yellow area in Fig. 2). Its duty cycle is controlled to assign the reference value v_7^* to v_{C_7}, forcing the battery to provide/absorb a desired amount of power, in a smooth way that maximizes its lifetime. This reference value is given by the higher controller not considered in the present paper, and is taken as constant during the time period T. It must to be noticed that the reference in terms of voltage v_7^* has the same meaning as a reference in terms of power. Indeed, it is easy to relate the power to the voltage of the DC grid and the current coming from the battery [10]. The DC/DC converter connecting the supercapacitor to the DC grid is a bidirectional buck-boost (blue area in Fig. 2). The target is to control the capacitor's voltage directly connected to the grid, v_{10}, for maintaining a desired reference value v_{15}^* for the DC grid. According to the supercapacitor's target to maintain voltage grid stability, it is not expected to be completely charged or discharged. As already stated, the high level controller is supposed to calculate the reference for the power coming from the battery in a way such that the state of charge of the supercapacitors is 50% of its operability (about 75% of maximum voltage) at the beginning of each time interval (this is the best starting point for efficiency reasons) without taking into account unmodeled disturbances [8].

2.1. Grid modelling

Here the mathematical model is given, based on power electronics averaging technique:

$$\begin{cases} \dot{v}_{C_1} = \frac{1}{R_1 C_1}(v_{PV} - v_{C_1}) - \frac{1}{C_1} i_{L_3} \\ \dot{v}_{C_2} = \frac{1}{R_2 C_2}(v_{C_{12}} - v_{C_2}) + \frac{1}{C_2} i_{L_3}(1 - u_1) \\ \dot{i}_{L_3} = \frac{1}{L_3} v_{C_1} - \frac{1}{L_3} v_{C_2}(1 - u_1) - \frac{R_{01}}{L_3} i_{L_3} \\ \dot{v}_{C_4} = \frac{1}{R_4 C_4}(v_T - v_{C_4}) - \frac{1}{C_4} i_{L_6} \\ \dot{v}_{C_5} = \frac{1}{R_5 C_5}(v_{C_{12}} - v_{C_5}) + \frac{1}{C_5} i_{L_6}(1 - u_2) \\ \dot{i}_6 = \frac{1}{L_6} v_{C_4} - \frac{1}{L_6} v_{C_5}(1 - u_2) - \frac{R_{04}}{L_6} i_{L_6} \\ \dot{v}_{C_7} = \frac{1}{R_7 C_7}(v_B - v_{C_7}) - \frac{1}{C_7} i_{L_9} \\ \dot{v}_{C_8} = \frac{1}{R_8 C_8}(v_{C_{12}} - v_{C_8}) + \frac{1}{C_8} i_{L_9}(1 - u_3) \\ \dot{i}_{L_9} = \frac{1}{L_9} v_{C_7} - \frac{1}{L_9} v_{C_8}(1 - u_3) - \frac{R_{07}}{L_9} i_{L_9} \\ \dot{v}_{C_{10}} = \frac{1}{R_{10} C_{10}}(v_{C_{12}} - v_{C_{10}}) + \frac{1}{C_{10}} i_{L_{11}} \\ \dot{i}_{L_{11}} = \frac{1}{L_{11}} V_S u_4 - \frac{R_{08}}{L_{11}} i_{L_{11}} - \frac{1}{L_{11}} v_{C_{10}} \\ \dot{v}_{C_{12}} = \frac{v_{C_2} - v_{C_{12}}}{R_2 C_{12}} + \frac{v_{C_5} - v_{C_{12}}}{R_5 C_{12}} + \frac{v_{C_8} - v_{C_{12}}}{R_8 C_{12}} - \frac{v_{C_{12}}}{R_L C_{12}} \end{cases} \quad (1)$$

The state $x(t)$ is composed by 15 variables, where the v_{C_i}, $i = \{1, 2, 4, 5, 7, 8, 10, 12\}$, represent the voltage of capacitors C_i, while i_{L_j}, $j = \{3, 6, 9, 11\}$, are the currents in the inductors L_j. The dynamical behaviour of the system is in the form

$$\dot{x}(t) = f(x(t)) + g(x(t), u(t), d(t)) + h(x(t), d(t)) \quad (2)$$

where u is the control vector and d describes the disturbances acting on the system.

$$u = \begin{bmatrix} u_1 & u_2 & u_3 & u_4 \end{bmatrix}^T \quad (3)$$

$$d = \begin{bmatrix} v_{PV} & v_T & v_B & v_S & R_L \end{bmatrix}^T \quad (4)$$

where the values of the capacitors, resistances and the inductors are known and positive. $v_{PV} > 0$, $v_B > 0$, $v_S > 0$ are positive values of the PV array,the battery and the supercapacitor voltages, while $v_T > 0$ is the voltage of the braking energy recovery system. The control inputs in u are the duty cycles of the converters.

3. Control strategy

Let us consider the introduced hypothesis about the higher level controller providing references for power balance and about the proper sizing of the devices. Then, given the references that allow power balance in steady-state with respect to the load R_L at the desired voltage grid, it is possible to state that:

Theorem

Control inputs u_1, u_2, u_3, u_4, exist such that the system in (1) is asymptotically stable in an operating region in closed loop around the equilibrium point x^e ensuring power balance, where x^e is

$$x^e = [v_1^* \ v_2^e \ i_3^e \ v_4^* \ v_5^e \ i_6^e \ v_7^* \ v_8^e \ i_9^e \ v_{12}^* \ 0 \ v_{12}^*]^T$$

with

$$v_i^e = \frac{1}{2}\left(v_{C_{12}}^* + \sqrt{{v_{C_{12}}^*}^2 + 4 R_i C_i \Delta_i}\right), \ i = \{2, 5, 8\} \quad (5)$$

$$\Delta_2 = \frac{1}{R_1 C_2}(v_{PV} - v_1^*)\left[v_1^* - \frac{R_{01}}{R_1}(v_{PV} - v_1^*)\right] \quad (6)$$

$$\Delta_5 = \frac{1}{R_4 C_5}(v_T - v_4^*)\left[v_4^* - \frac{R_{04}}{R_4}(v_T - v_4^*)\right] \quad (7)$$

$$\Delta_8 = \frac{1}{R_7 C_8}(v_B - v_7^*)\left[v_7^* - \frac{R_{07}}{R_7}(v_B - v_7^*)\right] \quad (8)$$

$$i_3^e = \frac{v_{PV} - v_1^*}{R_1}, \quad i_6^e = \frac{v_T - v_4^*}{R_4}, \quad i_9^e = \frac{v_B - v_7^*}{R_7} \quad (9)$$

Proof

The proof is based on a composition of Lyapunov functions [11], [10], [12]. The control inputs u_1, u_2, u_3, are designed to implement a feedback stabilizing PI controller to the converters such that a Lyapunov function for each dynamics involved in power reference tracking is found, i.e. $W_{1,3}$, $W_{4,6}$, $W_{7,9}$,

are positive definite and have negative definite time derivates $\dot{W}_{1,3}$, $\dot{W}_{4,6}$, $\dot{W}_{7,9}$, ensuring asymptotic stability. The control inputs are

$$u_1 = \frac{1}{v_{C_2}} \left[-v_{C_1} + v_{C_2} + R_{01} i_{L_3} - L_3 w_1 \right] \quad (10)$$

$$u_2 = \frac{1}{v_{C_5}} \left[-v_{C_4} + v_{C_5} + R_{04} i_{L_6} - L_6 w_2 \right] \quad (11)$$

$$u_3 = \frac{1}{v_{C_8}} \left[-v_{C_7} + v_{C_8} + R_{07} i_{L_9} - L_9 w_3 \right] \quad (12)$$

with

$$w_1 = K_3(i_{L_3} - z_3) + \overline{K}_3 \alpha_3 - C_1 \overline{K}_1 K_1^{\alpha} (v_{C_1} - v_1^*) + \\ + \left(C_1 K_1 - \frac{1}{R_1} \right) \left(K_1 (v_{C_1} - v_1^*) + \overline{K}_1 \alpha_1 \right) \quad (13)$$

$$w_2 = K_6(i_{L_6} - z_6) + \overline{K}_6 \alpha_6 - C_4 \overline{K}_4 K_4^{\alpha} (v_{C_4} - v_4^*) + \\ + \left(C_4 K_4 - \frac{1}{R_4} \right) \left(K_4 (v_{C_4} - v_4^*) + \overline{K}_4 \alpha_4 \right) \quad (14)$$

$$w_3 = K_9(i_{L_9} - z_9) + \overline{K}_9 \alpha_9 - C_7 \overline{K}_7 K_7^{\alpha} (v_{C_7} - v_7^*) + \\ + \left(C_7 K_7 - \frac{1}{R_7} \right) \left(K_7 (v_{C_7} - v_7^*) + \overline{K}_7 \alpha_7 \right) \quad (15)$$

$$z_3 = \frac{1}{R_1}(v_{PV} - v_{C_1}) + C_1 K_1 (v_{C_1} - v_1^*) + C_1 \overline{K}_1 \alpha_1 \quad (16)$$

$$z_6 = \frac{1}{R_4}(v_T - v_{C_4}) + C_4 K_4 (v_{C_4} - v_4^*) + C_4 \overline{K}_4 \alpha_4 \quad (17)$$

$$z_9 = \frac{1}{R_7}(v_B - v_{C_7}) + C_7 K_7 (v_{C_7} - v_7^*) + C_7 \overline{K}_7 \alpha_7 \quad (18)$$

where, for $i = \{1, 3, 4, 6, 7, 9\}$, the positive gains K_i, $\overline{K}_i$, K_i^{α}, have to be properly chosen and α_i are integral terms assuring zero error in steady state:

$$\dot{\alpha}_1 = K_1^{\alpha}(v_{C_1} - v_1^*) \qquad \dot{\alpha}_3 = K_3^{\alpha}(i_{L_3} - z_3) \quad (19)$$

$$\dot{\alpha}_4 = K_4^{\alpha}(v_{C_4} - v_4^*) \qquad \dot{\alpha}_6 = K_6^{\alpha}(i_{L_6} - z_6) \quad (20)$$

$$\dot{\alpha}_7 = K_7^{\alpha}(v_{C_7} - v_7^*) \qquad \dot{\alpha}_9 = K_9^{\alpha}(i_{L_9} - z_9) \quad (21)$$

Because of the obtained stable feedback linearized systems, it is possible to calculate positive definite Lyapunov functions $W_{1,3}$, $W_{4,6}$, $W_{7,9}$, for the augmented systems considering also the integral error dynamics, such that their time derivative are negative definite [10]. Then $W_{1,3} > 0$, $W_{4,6} > 0$, $W_{7,9} > 0$, such that $\dot{W}_{1,3} < 0$, $\dot{W}_{4,6} < 0$, $\dot{W}_{7,9} < 0$.

In order to respect voltage stability and to have robustness with respect to the strong power variation coming from the PV array and the braking energy recovery system, the control input of the supercapacitor connected DC/DC converter is calculated. Its duty is to stabilize the grid voltage and the system interconnection. Then Lyapunov functions for the remaining dynamics are calculated and the stabilizing control law u_4 is obtained in order to have $W_{2,5,8,12} > 0$ and $W_{10,11} > 0$ such that $\dot{W}_{2,5,8,12} \leq 0$ and $W_{10,11} < 0$. To find a proper control action, the $W_{2,5,8,12}$ is defined as

$$W_{2,5,8,12} = \frac{C_2}{2} e_2^2 + \frac{C_5}{2} e_5^2 + \frac{C_8}{2} e_8^2 + \frac{C_{12}}{2} v_{C_{12}}^2 \quad (22)$$

where the errors e_2, e_5, e_8, are the difference between the dynamics v_{C_2}, v_{C_5}, v_{C_8}, and their equilibrium points;

$$e_2 = v_{C_2} - v_2^e \,,\; e_5 = v_{C_5} - v_5^e \,,\; e_8 = v_{C_8} - v_8^e \quad (23)$$

According to this change of variables, it is then possible to rewrite the equations as

$$\begin{cases} \dot{e}_2 = \frac{1}{R_2 C_2}(v_{C_{12}} - e_2 - v_2^e) + \frac{1}{C_2} i_{L_3}(1 - u_1) \\ \dot{e}_5 = \frac{1}{R_5 C_5}(v_{C_{12}} - e_5 - v_5^e) + \frac{1}{C_5} i_{L_6}(1 - u_2) \\ \dot{e}_8 = \frac{1}{R_8 C_8}(v_{C_{12}} - e_8 - v_8^e) + \frac{1}{C_8} i_{L_9}(1 - u_3) \\ \dot{v}_{C_{12}} = \frac{e_2 + v_2^e - v_{C_{12}}}{R_2 C_{12}} + \frac{e_5 + v_5^e - v_{C_{12}}}{R_5 C_{12}} + \\ \qquad + \frac{e_8 + v_8^e - v_{C_{12}}}{R_8 C_{12}} - \frac{v_{C_{12}}}{R_L C_{12}} \end{cases} \quad (24)$$

Then the time derivative is

$$\dot{W}_{2,5,8,12} = -\frac{1}{R_2} e_2^2 - \frac{1}{R_5} e_5^2 - \frac{1}{R_8} e_8^2 + \\ + \Psi_2 + \Psi_5 + \Psi_8 + \Psi_{12} + \\ + \frac{v_{C_{12}}}{R_{10}}(v_{C_{10}} - v_{C_{12}}) \quad (25)$$

where

$$\Psi_2 = e_2 \left(\frac{1}{R_2}(v_{C_{12}} - v_2^e) + i_{L_3}(1 - u_1) \right) \quad (26)$$

$$\Psi_5 = e_5 \left(\frac{1}{R_5}(v_{C_{12}} - v_5^e) + i_{L_6}(1 - u_2) \right) \quad (27)$$

$$\Psi_8 = e_8 \left(\frac{1}{R_8}(v_{C_{12}} - v_8^e) + i_{L_9}(1 - u_3) \right) \quad (28)$$

$$\Psi_{12} = v_{C_{12}} \left(\frac{e_2 + v_2^e - v_{C_{12}}}{R_2} + \frac{e_5 + v_5^e - v_{C_{12}}}{R_5} \right) + \quad (29)$$

$$+ v_{C_{12}} \left(\frac{e_8 + v_8^e - v_{C_{12}}}{R_8} \right) - \frac{v_{C_{12}}^2}{R_L}$$

In equation (25) the voltage $v_{C_{10}}$ must be seen as the control input; it can be properly chosen to obtain a desired form for $\dot{W}_{2,5,8,12}$. Considering $K_{10} > 0$, let us then define the reference z_{10} for $v_{C_{10}}$ as

$$z_{10} = -R_{10} \frac{1}{v_{C_{12}}} \left[\Psi_2 + \Psi_5 + \Psi_8 + \Psi_{12} \right] + \quad (30)$$

$$- \frac{R_{10}}{v_{C_{12}}} \left[{v_{12}^*}^2 - 2 v_{C_{12}} v_{C_{12}}^* \right] - \frac{R_{10} K_{10}}{v_{C_{12}}} \left[v_{C_{12}} - v_{12}^* \right]^2 \quad (31)$$

When $v_{C_{10}}$ reaches its reference value, then $\dot{W}_{2,5,8,12}$ results to be negative semidefinite. To prove asymptotic stability the set Ω is considered: it is the largest invariant set of the set E of all points where the Lyapunov function is not decreasing. Ω is shown to contain an unique point.

$$\dot{W}_{2,5,8,12} = -\frac{1}{R_2} e_2^2 - \frac{1}{R_5} e_5^2 - \frac{1}{R_8} e_8^2 + \quad (32)$$

$$- \left(\frac{1}{R_{10}} + K_{10} \right) \left[v_{C_{12}} - v_{12}^* \right]^2 \leq 0$$

$$\Omega = \{ (e_2, e_5, e_8, v_{C_{12}}) \, : \, v_{C_2} = v_2^e, \quad (33)$$

$$v_{C_5} = v_5^e, v_{C_8} = v_8^e, \, v_{C_{12}} = v_{12}^* \} =$$

$$= \{ (0, 0, 0, v_{15}^*) \}$$

LaSalle's theorem can be applied to $\dot{V}_{2,5,8,12}$ to prove asymptotic stability around the desired DC grid voltage level. To assign the reference z_{10} the control input u_4 is calculated again by backstepping technique. To this purpose, the candidate Lyapunov function $W_{10,11}$ is in the form of

$$W_{10,11} = \frac{C_{10}}{2} (v_{C_{10}} - z_{10})^2 + \frac{L_{11}}{2} (i_{L_{11}} - z_{11})^2 \quad (34)$$

where z_{11} is the reference for $i_{L_{11}}$ and $K_{10} > 0$, defined as

$$z_{10} = -\frac{1}{C_{10}} (v_{C_{15}} - v_{C_{10}}) + C_{10} \dot{z}_{10} - K_{10} (v_{C_{10}} - z_{10}) \quad (35)$$

with $\dot{z}_{10}$ being the time derivative of z_{10}. Then the control input u_4 defined as

$$u_4 = \frac{1}{V_S} (R_{08} i_{L_{11}} + v_{C_{10}}) + L_{11} \dot{z}_{11} - K_{11} (i_{L_{11}} - z_{11})) \quad (36)$$

where $\dot{z}_{11}$ is the time derivative of z_{11} and $K_{11} > 0$, define a negative definite $\dot{W}_{10,11}$:

$$\dot{W}_{10,11} = -K_{10} (v_{C_{10}} - z_{10})^2 - K_{11} (i_{L_{11}} - z_{11})^2 \, < 0 \quad (37)$$

Then a positive definite Lyapunov function $W > 0$ with semidefinite negative time derivative $\dot{W} \leq 0$ ensuring asymptotic voltage stability and power balance is introduced.

$$W = W_{1,3} + W_{4,6} + W_{7,9} + W_{2,5,8,12} + W_{10,11} \quad (38)$$

$$\dot{W} = \dot{W}_{1,3} + \dot{W}_{4,6} + \dot{W}_{7,9} + \dot{W}_{2,5,8,12} + \dot{W}_{10,11} \quad (39)$$

4. Simulations

In this section a simulation of the proposed scheme and the relative control action is introduced: the Matlab toolbox SimPower has been used for the implementation. The values of the converters are introduced in Table 2, while the considered ratings are in Table 1.

Simulation time is 10 s. In the considered scenario a constant load is assumed; the needed power to match power balance is provided by the PV array, the battery and the energy recovered by the train braking. The from the battery power coming will be bounded by the high level controller by imposing a limitation on the power variation on the battery. The high level controller will then provide a reference to the local controller of the battery connected DC/DC converter such that the storage device will not deteriorate its lifetime. The instantaneous power balance will then be provided by the supercapacitor.

Fig. 3 shows the irradiance the PV array is affected by: according to it, a current is generated by the PV array (see Fig. 4). During the considered scenario, a train is supposed to start braking at second 3 and completely stop at second 8; during the braking time, the energy recovery system generates the current introduced in Fig. 4.

Fig. 5 depicts the load behaviour. The resulting needed power to match power balance between the

Table 1: Ratings

Branch	Rating
PV	1 MW
Train	1 MW
Battery	1 MW
Supercapacitor	1 MW
Load	1 MW
Grid nominal voltage	1000 V

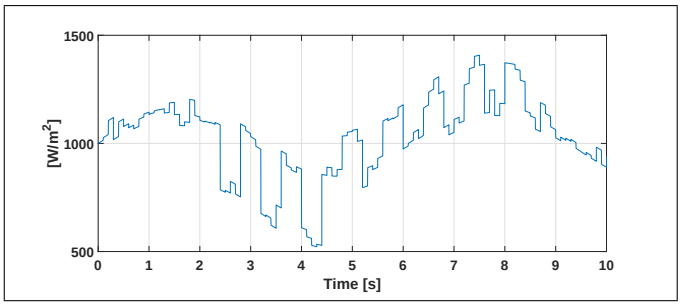

Figure 3: The irradiance on the PV array.

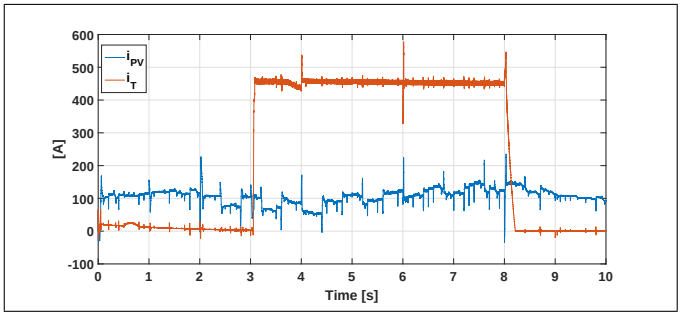

Figure 4: The current generated by the PV array, i_{PV}, and the one by the train braking recovery system, i_T.

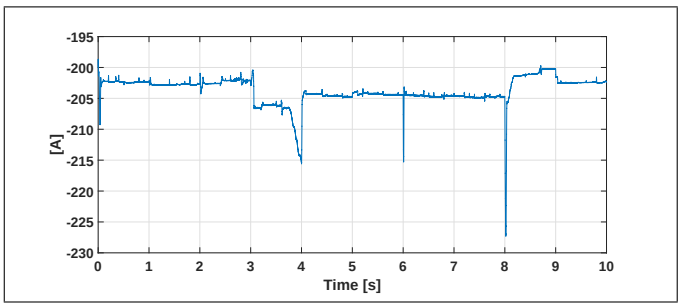

Figure 5: The current consumed by the load.

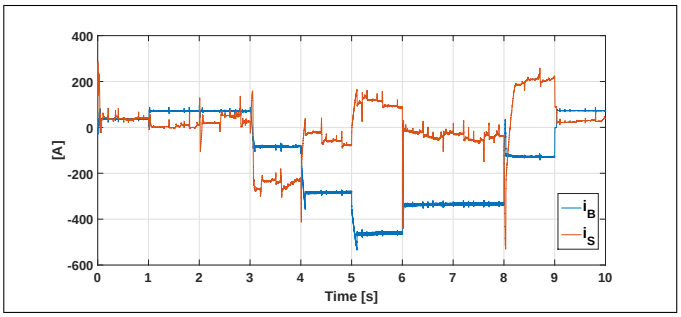

Figure 6: The current absorbed/generated by the supercapacitor, i_S, and by the battery, i_B.

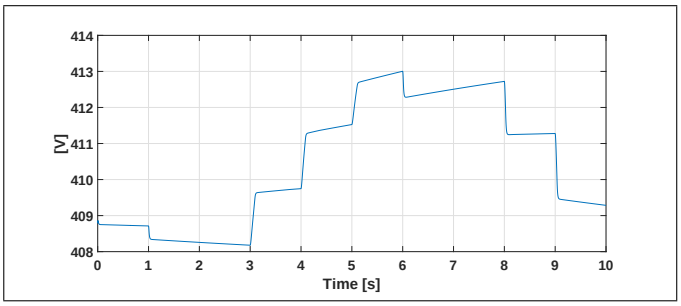

Figure 7: The voltage of the battery.

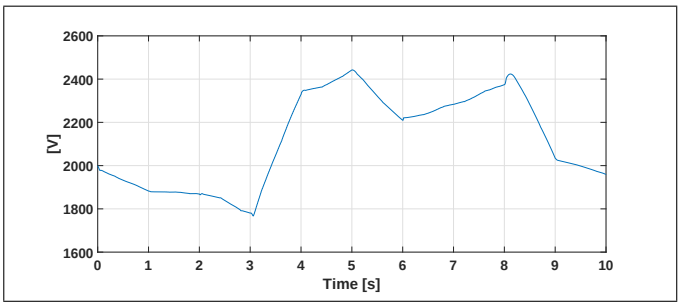

Figure 8: The voltage of the supercapacitor.

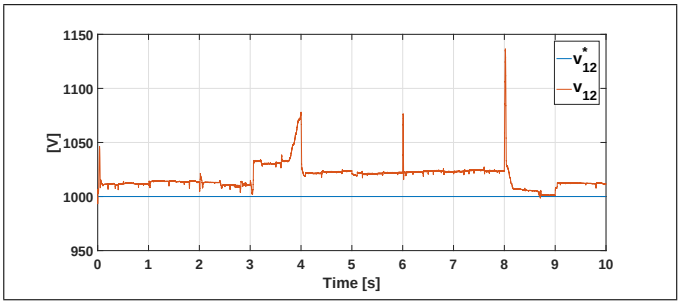

Figure 9: The voltage of the DC grid compared to its reference.

load and the renewables is then provided/taken by the supercapacitor and the battery: such currents are introduced in Fig. 6. The battery current profile is a trade-off between the desired current to be absorbed/provided in order to meet power balance and the necessity to preserve battery lifetime with a smooth charge/discharge ratio. According to these currents, the storage devices will have voltage variations; they are shown in Fig. 7 and 8. During the entire time, the supercapacitor takes the duty to absorb/provide the extra/missing power, as a consequence to its main duty to control voltage stability. The supercapacitor dynamics permits an acceptable voltage variation; a dedicated high level controller will allow initial voltage restoration in a desired time interval. A slower discharge is presented in the battery, due to the different nature and size of the device.

The control action introduced in Section 3 properly maintains the grid voltage in the desired range of about 10% of the nominal value of $1000\,V$, as stated in Fig. 9. There is only a peak exceeding this range, and it is due to the fast response that is asked to the braking energy recovery system. Then it is possible to state that the main result of the paper is accomplished, and that the DC microgrid is controlled in an efficient way. Indeed, the dynamics of the storage devices associated to the one of the current generated by the braking generates a perturbation of 2.85 $kV/\mu s$ (from Fig. 9) and 0.562 $A/\mu s$ (from Fig. 5). This perturbation will not affect the dynamics of the storage devices or of the grid, but it could influence the converters in transient time. A better regulation of the controllers could avoid a dedicated EMI study. Also, an action dedicated to smooth the slope of the current generated by the braking energy recovering system can be considered: indeed, the high variation of power is a main cause of the perturbation acting on the DC grid voltage. A trade-off situation can be chosen with respect to the maximum energy recovery and to reasonable voltage variations.

5. Conclusions

In this paper a control scheme dedicated to maintain voltage and power stability of a DC microgrid is introduced. Such scheme is applied to a DC Microgrid which includes two intermittent renewable sources and two storage systems acting in different time scales. The proposed scheme takes the opportunity to use a braking energy recovery system added to the the integration of renewables.

Thanks to the mixed storage (battery and supercapacitor), the impact of the voltage variation is bounded and leads to a better station DC grid stabilization. Simulation results show the effectiveness of the proposed control analysis. Future works will use the developed technique to detail limitations due to physical components.

Table 2: Grid parameters.

Par.	Value	Par.	Value	Par.	Value
C_1	100 mF	C_2	10 mF	L_3	33 mH
R_{01}	10 mΩ	R_{02}	10 mΩ	R_1	100 mΩ
R_2	100 mΩ	C_4	100 mF	C_5	10 mF
R_{04}	10 mΩ	R_{05}	10 mΩ	R_4	100 mΩ
R_5	10 mΩ	L_6	33 mH	C_8	10 mF
C_7	100 mF	R_7	100 mΩ	R_8	10 mΩ
L_9	33 mH	R_{07}	10 mΩ	R_{08}	10 mΩ
L_{11}	3.3 mH	R_{010}	10 mΩ	R_{011}	10 mΩ
C_{10}	10 mF	R_{10}	100 mΩ	C_{12}	0.1 mF
R_L	5 Ω				

6. References

[1] L. E. Zubieta. Are microgrids the future of energy?: DC microgrids from concept to demonstration to deployment. *IEEE Electrification Magazine*, 4(2):37–44, 2016.

[2] T. Dragicevic, J.C. Vasquez, J.M. Guerrero, and D. Skrlec. Advanced LVDC Electrical Power Architectures and Microgrids: A step toward a new generation of power distribution networks. *Electrification Magazine, IEEE*, 2(1):54–65, 2014.

[3] T. Dragicevic, X. Lu, J.C. Vasquez, and J.M. Guerrero. DC Microgrids-Part II: A Review of Power Architectures, Applications, and Standardization Issues. *Power Electronics, IEEE Transactions on*, 31(5):3528–3549, 2016.

[4] S. K. Chaudhary, J. M. Guerrero, and R. Teodorescu. Enhancing the Capacity of the AC Distribution System Using DC Interlinks;A Step Toward Fu-

ture DC Grid. *IEEE Transactions on Smart Grid*, 6(4):1722–1729, July 2015.

[5] L. Galai Dol and A. de Bernardinis. AC or DC grid for railway stations? In *PCIM Europe 2016; International Exhibition and Conference for Power Electronics, Intelligent Motion, Renewable Energy and Energy Management*, pages 1–8, May 2016.

[6] H. Farhangi. The path of the smart grid. *Power and Energy Magazine, IEEE*, 8(1):18–28, January 2010.

[7] D.E. Olivares, A. Mehrizi-Sani, A.H. Etemadi, C.A. Canizares, R. Iravani, M. Kazerani, A.H. Hajimiragha, O. Gomis-Bellmunt, M. Saeedifard, R. Palma-Behnke, G.A. Jimenez-Estevez, and N.D. Hatziargyriou. Trends in microgrid control. *Smart Grid, IEEE Transactions on*, 5(4):1905–1919, July 2014.

[8] Alessio Iovine, Gilney Damm, Elena De Santis, and Maria Domenica Di Benedetto. Management Controller for a DC MicroGrid integrating Renewables and Storages. In *20th IFAC World Congress on International Federation of Automatic Control (IFAC 2017)*, Toulouse, France, 2017.

[9] E. Jimenez, M. Jimenez Carrizosa, A. Benchaib, G. Damm, and F. Lamnabhi-Lagarrigue. A new generalized power flow method for multi connected DC grids. *International Journal of Electrical Power and Energy Systems*, 74:329 – 337, 2016.

[10] A. Iovine, S. B. Siad, G. Damm, E. De Santis, and M. D. Di Benedetto. Nonlinear Control of a DC MicroGrid for the Integration of Photovoltaic Panels. *IEEE Transactions on Automation Science and Engineering*, to appear.

[11] P. Kundur, J. Paserba, V. Ajjarapu, G. Andersson, A. Bose, C. Canizares, N. Hatziargyriou, D. Hill, A. Stankovic, C. Taylor, T. Van Cutsem, and V. Vittal. Definition and classification of power system stability IEEE/CIGRE joint task force on stability terms and definitions. *Power Systems, IEEE Transactions on*, 19(3):1387–1401, Aug 2004.

[12] A. Iovine, S. B. Siad, G. Damm, E. De Santis, and M. D. Di Benedetto. Nonlinear control of an AC-connected DC MicroGrid. In *IECON 2016 - 42nd Annual Conference of the IEEE Industrial Electronics Society*, pages 4193–4198, Oct 2016.

[13] R. R. Pecharroman, A. Lopez-Lopez, A. P. Cucala, and A. Fernandez-Cardador. Riding the Rails to DC Power Efficiency: Energy efficiency in dc-electrified metropolitan railways. *IEEE Electrification Magazine*, 2(3):32–38, Sept 2014.